

A fossil oceanic lithosphere preserved inside a continent

Shucheng Wu^{1*}, Yingjie Yang^{2†}, Yixian Xu^{3†}, Juan Carlos Afonso^{1,4} and Anqi Zhang²¹Department of Earth and Environmental Sciences, Macquarie University, North Ryde, NSW 2109, Australia²Department of Earth and Space Sciences, Southern University of Science and Technology, Shenzhen 518055, China³School of Earth Sciences, Zhejiang University, Hangzhou 310027, China⁴Faculty of Geo-Information Science and Earth Observation (ITC), University of Twente, 7514 AE Enschede, Netherlands

ABSTRACT

The recycling of oceanic lithosphere into the deep mantle at subduction zones is one of the most fundamental geodynamic processes on Earth. During the closure of an ocean, ancient oceanic slabs are thought to be consumed entirely in subduction zones due to their negative buoyancy. Yet, it is recently suggested that small pieces of oceanic slabs could be trapped along paleo-subduction zones. What remains far more enigmatic is whether significant portions of paleo-oceanic lithosphere could eventually avoid the fate of subduction and be accreted to continental lithosphere, thus contributing to continental growth through time. We present seismic evidence for a preserved paleo-oceanic lithosphere beneath the Junggar region in northwestern China. We show that unsubducted oceanic lithosphere in the West Junggar has been preserved beneath the Junggar Basin, becoming a piece of the Eurasian continent. This scenario is likely to have occurred in other continents throughout Earth's history, providing an additional and commonly underestimated contribution to the growth of continental lithosphere.

INTRODUCTION

The subduction of cold and dense oceanic lithosphere, which pulls the attached oceanic plate toward the trench and causes mantle convection, is thought to provide the main driving force for plate motions (Forsyth and Uyeda, 1975). A common postulate of plate tectonics and the Wilson cycle is that oceanic plates are eventually consumed entirely in a subduction zone, occasionally leaving only small fragments of oceanic crust and uppermost mantle in ophiolitic belts (Dewey, 2003; Dilek and Furnes, 2011). Yet, a few recent studies have shown that complete portions of ancient oceanic slabs can also be preserved along paleo-subduction boundaries after subduction halts (e.g., Wang et al., 2013; Schiffer et al., 2014; Xu et al., 2020). Moreover, a recent study based on the analysis of magnetic anomalies indicated that an old oceanic crust (~340 m.y. old) is preserved in the eastern Mediterranean Sea (Granot, 2016),

suggesting that under certain conditions, ancient oceanic lithosphere can avoid subduction for hundreds of millions of years. All this raises the important question of whether significant portions of unsubducted oceanic lithosphere could have escaped subduction and accreted to continental plates through Earth's history.

In this context, recent studies of borehole samples have suggested that the Junggar Basin (JB) in central Asia (Fig. 1) may be underlain by Paleozoic oceanic crustal fragments (Zheng et al., 2007; Xu et al., 2013). This foreland basin is located in the southern margins of the Central Asian orogenic belt and is surrounded by a series of Paleozoic ophiolitic belts and granitoids (Fig. 1). Our previous studies using magnetotelluric (Xu et al., 2016) and ambient noise data (Wu et al., 2018) suggested that a fossil oceanic slab might be preserved along a paleo-subduction zone in the western JB. However, although the model of Wu et al. (2018) delineated the top of a northwestward-dipping oceanic slab beneath the West Junggar, the resolution was limited to depths shallower than 30 km and the model could not characterize the nature of the deep lithosphere in the adjacent interior of the JB. High-resolution tomography of the shallow mantle is therefore necessary to elucidate

whether the paleo-oceanic lithospheric mantle is still attached and trapped inside the continental lithosphere or completely removed and recycled into the deep mantle.

In this study, we provide new seismic evidence for a preserved segment of oceanic lithosphere beneath the JB. We deployed a seismic array across the region to build a high-resolution three-dimensional (3-D) upper mantle velocity model. Our new 3-D velocity model sheds light on the origin and fate of trapped oceanic plates and their role in the growth of continental lithosphere since the beginning of plate tectonics.

PHASE VELOCITY MAPS

We collected one year of vertical component seismic data recorded by our seismic array, which consists of 49 stations (Fig. 1). We then applied ambient noise tomography (ANT) to continuous noise data to obtain phase velocity maps at 6–30 s periods and applied two-plane wave tomography (TPWT) to teleseismic surface waves to obtain phase velocity maps at 25–150 s periods. The data processing for ANT (Bensen et al., 2007) and TPWT (Yang and Forsyth, 2006) is detailed in the Supplemental Material¹. Phase velocity maps from ANT and TPWT at several selected periods are shown in Figure 2, together with a comparison of the phase velocities generated by the two different methods at the overlapping period of 28 s. Overall, phase velocity maps generated by the two methods agree well with each other at overlapped periods (Fig. 2F). At shorter periods (<20 s), we observe a significant low-velocity zone beneath the JB, in comparison to high-velocity anomalies in the mountainous areas. At longer periods (>50 s), the overall velocity perturbations become smaller, showing high velocities beneath the western JB and low velocities in the center of the West Junggar.

*Current address: Division of Mathematical Sciences, School of Physical and Mathematical Sciences, Nanyang Technological University, Singapore 637371, Singapore

†E-mails: yangyj@sustech.edu.cn; xyxian@zju.edu.cn

¹Supplemental Material. Detailed description of the seismic imaging methods and resolution analyses. Please visit <https://doi.org/10.1130/GEOL.S.21644651> to access the supplemental material, and contact editing@geosociety.org with any questions.

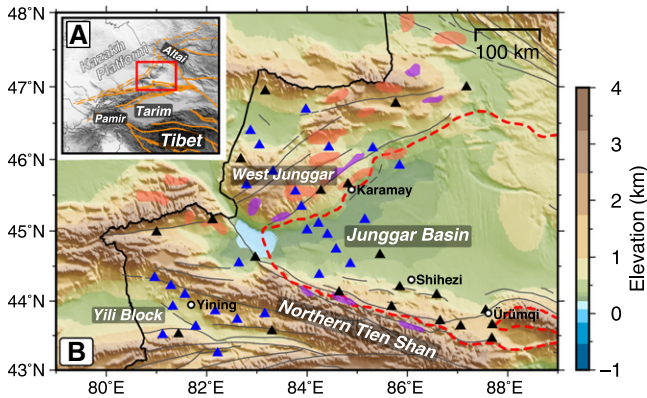


Figure 1. Topographic map of the Junggar region, northwestern China, with geologic features. (A) Location of the study region (red rectangle). Black and orange lines denote national borders and tectonic block boundaries, respectively. (B) Locations of seismic stations used in this study. Black and blue triangles represent 21 fixed stations from the China Earthquake Administration and 28 newly deployed stations, respectively. Major late

Paleozoic ophiolites and granitoids are indicated by violet and orange colors, respectively. Red dashed line and gray solid lines indicate the geomorphic boundary of the Junggar Basin and regional active faults, respectively. Major cities are shown as white circles.

3-D SHEAR VELOCITY MODEL

We then constructed a 3-D Vs model by inverting the phase velocities at periods of 6–150s (see the Supplemental Material). Figure 3 shows Vs perturbation maps at four depths and two profiles displaying absolute velocities. In the upper crust (Fig. 3A), the patterns of velocity anomalies correlate well with surface geology. A large triangle-shaped low-velocity zone (<2.8 km/s) dominates the entire JB down to depths in excess of 10 km, which corresponds to the thick sediments in the basin (Zhao et al., 2003). Conversely, high velocities are observed in the mid- to lower crust and in the uppermost mantle beneath the JB, whereas relatively low velocities are found beneath the West Junggar (Fig. 3). The high-velocity body in the uppermost mantle of the JB dips slightly toward the northwest, reaching a maximum depth

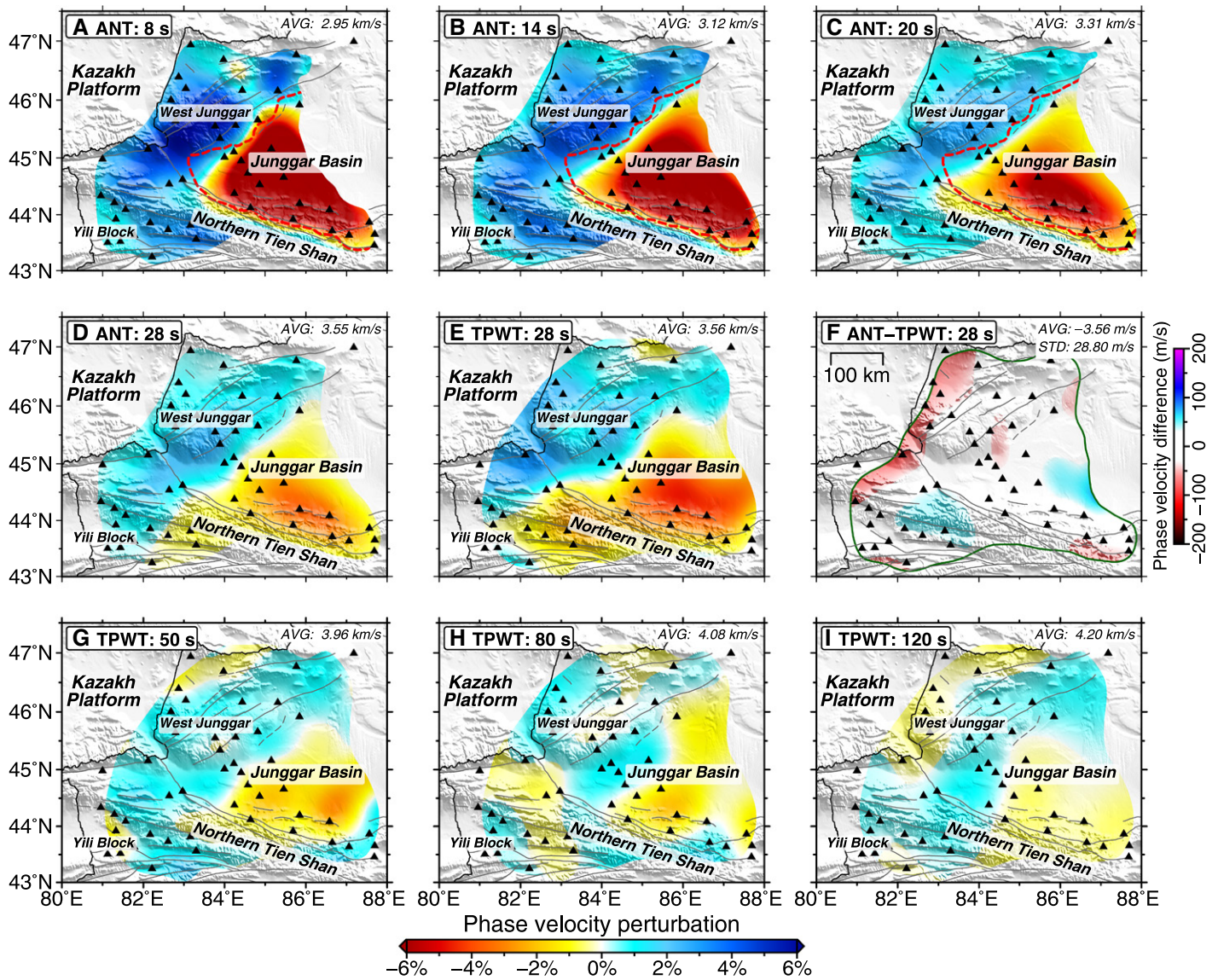


Figure 2. (A–E, G–I) Phase velocity maps from ambient noise tomography (ANT) (A–D) and two-plane wave tomography (TPWT) (E, G–I) at selected periods. Phase velocities are displayed as velocity perturbations with respect to average velocity (AVG) shown at the top right corner of each map. (F) Phase velocity difference map between ANT and TPWT at 28 s period. Mean (AVG) and one standard deviation (STD) of velocity difference are shown at the top right. Black triangles indicate seismic stations.

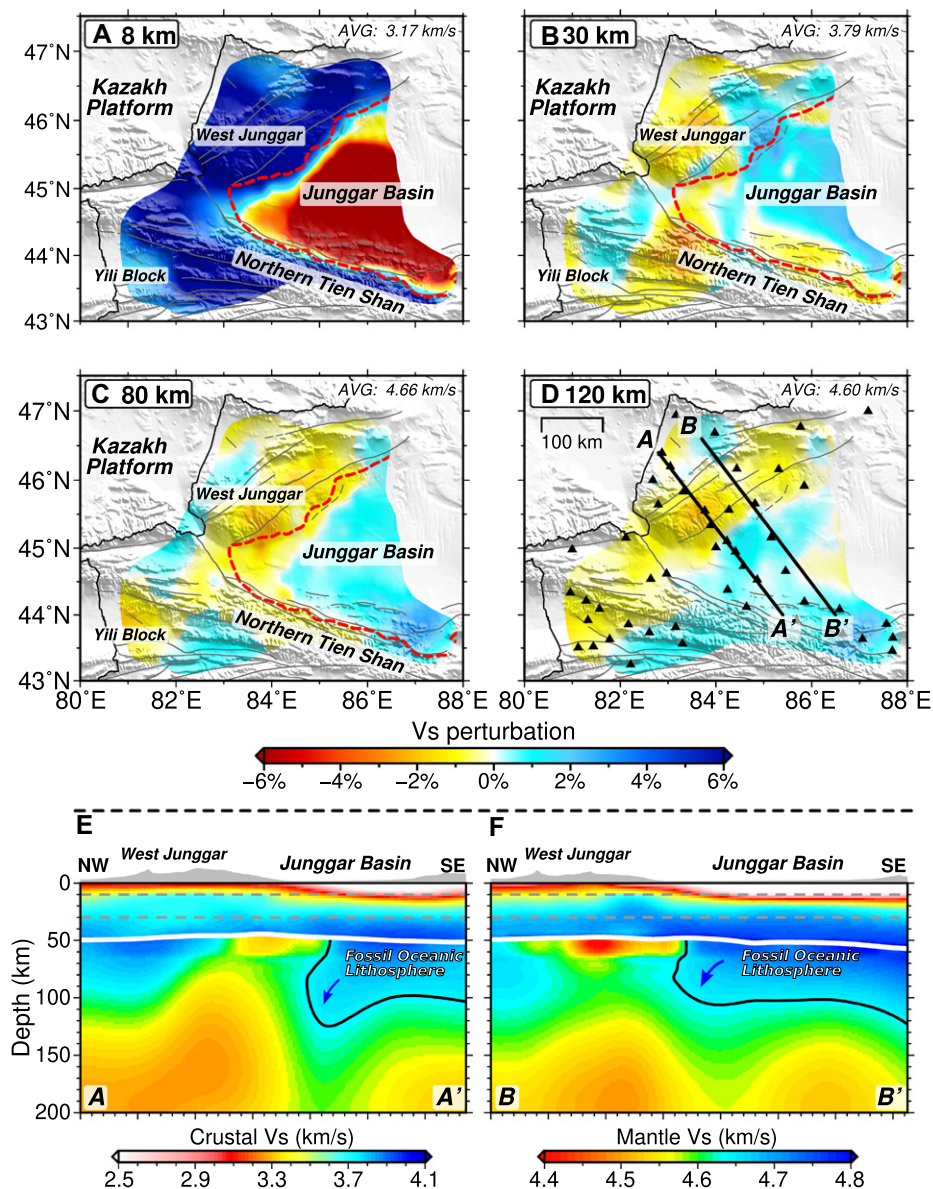


Figure 3. The final Vs model displayed as four horizontal velocity perturbation slices (A–D) and two vertical cross sections (E and F). Velocity perturbations in A–D are shown with respect to average Vs (AVG) labeled at the top right corner in each horizontal slice. Profiles of vertical transects and locations of seismic stations are shown in D as black lines and triangles, respectively. White bold lines in the transects indicate Moho interface, and black bold lines outline the extent of fossil oceanic lithosphere following the Vs contour of 4.65 km/s. Note that different color patterns are used to display the velocity of the crust and upper mantle in vertical cross sections.

of ~110–140 km beneath the westernmost parts of the basin. From there, it transitions abruptly into a tilted, low-velocity region beneath the West Junggar (Figs. 3E and 3F).

DISCUSSION AND CONCLUSION

The Nature of the High-Velocity Upper Mantle beneath the Junggar Basin

The nature of the JB lithosphere remains a contentious topic. The JB lithosphere is characterized by high seismic velocities (Fig. 3), and it has been previously interpreted as either a Precambrian microcontinent (Watson et al., 1987) or fragments of a Paleozoic oceanic plate (Chen and Jahn, 2004; Xu et al., 2013). In our

previous work, we found a northwest-dipping high-velocity body in the mid- to lower crust beneath the West Junggar (Wu et al., 2018). The observed Vs in the mid- to lower crust are considerably higher than those expected for continental crust but match well predicted velocities of metamorphosed mid-ocean ridge basalt (Wu et al., 2018) or metamorphosed mafic lower continental crust (Christensen, 1996). Given an oceanic geochemical signature of JB basement samples (e.g., Zheng et al., 2007), we believe that the high-velocity JB basement more likely originates from an old oceanic crust. Furthermore, a recent thermochemical study indicated that the physical properties of the lithospheric

mantle beneath the JB are more consistent with those expected in a cooling oceanic lithosphere (since ca. 270 Ma) rather than in typical Precambrian subcontinental mantle (Zhang et al., 2019). All of the above points to the possible preservation of a portion of the late Paleozoic oceanic lithosphere beneath the present-day JB.

In both the A–A' and B–B' profiles (Fig. 3D), a nearly flat body of high velocities is observed in the middle to lower crust and uppermost mantle beneath the JB (Figs. 3E and 3F; the bottom of the high-velocity body is outlined by the black 4.65 km/s velocity contour). Based on the geometry of the high-velocity body and evidence from the previous studies, we speculate that the high-velocity body beneath the JB represents a trapped portion of the ancient Junggar Ocean that has escaped complete subduction during the final amalgamation of the Central Asian orogenic belt. The geometry of the high-velocity body further suggests a northwest polarity of the late Paleozoic subduction beneath the West Junggar. We note that the depth extent of the high-velocity lid beneath the JB is much shallower than the present-day thermal lithosphere-asthenosphere boundary of 200–250 km (Zhang et al., 2019). This suggests that the high-velocity body may represent the depleted, dry, and faster paleo-oceanic lithosphere (Yang et al., 2007), whereas the lower portion of lithospheric mantle represents ancient sublithospheric mantle cooled after subduction termination (Zhang et al., 2019).

To further support our interpretation of this high-velocity body as a fossil segment of oceanic lithosphere, we calculated mantle seismic velocities following the thermal evolution after subduction termination. We note that no significant post-Paleozoic reheating or tectono-thermal events occurred in the region after the subduction ceased (Xu et al., 2020). Thus, if the JB lithosphere is a trapped portion of oceanic lithosphere surrounded by thicker continental lithosphere, we can assume that its thermal evolution after subduction cessation was mainly via conductive cooling. With this assumption, we can estimate the present-day temperature structure and use it to predict the associated Vs, which can then be compared with our 3-D Vs model. The age at which subduction ceased is important because it affects both the calculated temperature and the predicted velocity. Most previous studies have suggested that subduction in the West Junggar probably terminated at the end of the Permian, alongside the closure of the Paleo-Asian Ocean (e.g., Xiao et al., 2008; Zhang et al., 2021). Accordingly, we varied the age of subduction termination from 400 to 150 Ma in our calculation. Note that we assume a young initial age for the Permian slab based on evidence regarding the size of the Junggar Ocean and the subduction of a mid-ocean ridge in the Carboniferous (Tang et al., 2010; Yin et al., 2013). Details of the Vs calculation are described in the Supplemental Material.

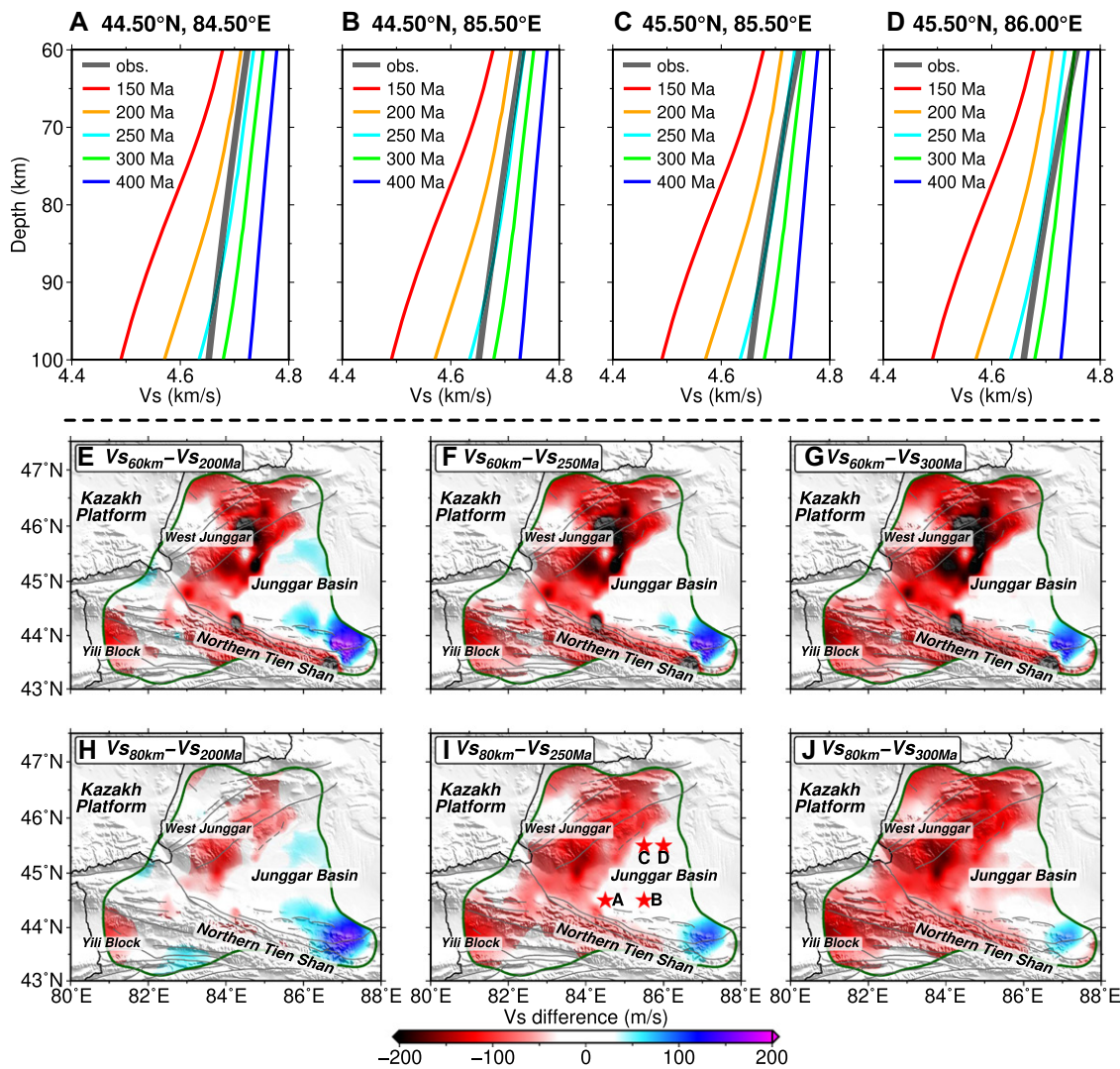


Figure 4. Comparisons between observed Vs (obs.) and predicted Vs from the half-space cooling model based on different cooling ages. (A–D) Comparisons of one-dimensional Vs for four selected grid nodes located in the Junggar Basin in northwestern China. Locations of these nodes are given in I. Gray bold lines denote observed Vs, whereas calculated age-dependent Vs are shown as color-coded lines. (E–J) Maps of Vs differences between observed Vs and calculated age-dependent ones at 60 and 80 km. The values of differences are indicated at the top left corner of each panel, where Vs_{60km} and Vs_{80km} refer to observed Vs at depths of 60 and 80 km, respectively, and Vs_{200Ma} , Vs_{250Ma} and Vs_{300Ma} refer to calculated Vs at a corresponding depth for a cooling age of 200, 250, or 300 Ma, respectively.

Figure 4 shows a comparison between predicted and observed Vs plotted as one-dimensional (1-D) profiles and as Vs difference maps at 60 and 80 km depth for the entire region. The comparisons of 1-D Vs profiles in four representative locations show that the uppermost mantle Vs beneath the JB agree well with those predicted for a subduction termination age of ca. 250–300 Ma (i.e., end of Permian; Figs. 4A–4D). The results in the Vs difference maps show that the same conclusion applies to the majority of the JB (white areas in Figs. 4F and 4I). The agreement between predicted and observed Vs for areas other than the JB is considerably poorer, which is expected given the fact that the model of oceanic lithosphere cooling does not represent the evolution of lithosphere beneath regions other than the JB.

Taken together with the previously identified fossil oceanic crustal fragments preserved in the mid- to lower crust (Zheng et al., 2007; Xu et al., 2013), the excellent agreement between predicted and observed lithospheric mantle Vs for cooling ages of ca. 250–300 Ma offers further support for the existence of rem-

nant late Paleozoic oceanic lithosphere preserved beneath the JB.

Survival of the Trapped Oceanic Lithosphere

It is generally thought that when oceanic lithosphere gets colder, it becomes gravitationally unstable and subducts into the deep mantle. One crucial question is how the trapped oceanic lithosphere could have survived beneath the JB without further subduction and/or destabilization.

Zhang et al. (2019) proposed that the oceanic basement of the JB was affected (i.e., thickened) by the presence of a plume, either during the generation of the oceanic crust in a “hot ride” setting or shortly after (as in modern oceanic plateaus). Regardless of the actual setting, the hot mantle temperatures resulted in extensive melting, which in turn created (1) an anomalously thick mafic crust, and (2) an ultra-depleted mantle residue in the uppermost mantle. As mentioned in previous sections herein, geophysical and geochemical evidence support both of these features beneath the JB. In addition, it is reported that a mid-ocean ridge was involved

in the subduction starting in the Carboniferous (Tang et al., 2010; Yin et al., 2013), indicating the late Paleozoic subducting slab might have been young and buoyant (Afonso et al., 2007). Numerical simulations indicate that these conditions would favor the accretion of the anomalous oceanic domain to the continent (Vogt and Gerya, 2014; Yan et al., 2021). Although further cooling would have increased the density of the preserved oceanic lithosphere, the thick oceanic crust, the low-density sedimentary cover, and the depleted oceanic lithospheric mantle all contributed to an overall neutral buoyancy, hindering further subduction and ensuring subsequent stability of the preserved oceanic lithosphere.

There are also several other factors that could have contributed to the preservation. Based on our model, the high-Vs anomaly disappears beneath the West Junggar at depths of more than ~110–140 km (Figs. 3E and 3F), indicating a discontinuation of the subducted slab, possibly as a result of slab break-off in the past. This is supported by numerical simulations, which demonstrate that slab break-off would have occurred when an oceanic plateau with a depleted mantle root

approached the trench (e.g., Yan et al., 2021). After the break-off, the unsubducted part of the oceanic lithosphere under the JB would have lost the main pulling force and subduction would have halted (Wang et al., 2013). These conditions would have resulted in a relatively stable system that tended to cool down conductively. The lack of later tectono-thermal perturbations in the region allowed the trapped Junggar oceanic plate to become the deposition center of thick sediments and, ultimately, part of the present-day continental lithosphere. We note that the evolution just described for the JB is reminiscent of the more general and recently proposed transmogriification process, where an oceanic basin gradually becomes “continental-like” lithosphere (Morgan and Vannucchi, 2022). However, with the constraint from our seismic imaging, more modeling work is needed to verify whether the JB is experiencing transmogriification, and if so, to which stage of the process its current structure belongs.

In summary, this work highlights a mechanism of continental growth that has been traditionally overlooked but that likely took place in many continental regions (e.g., Granot, 2016; Morgan and Vannucchi, 2022). Given that oceanic plates in the early Earth would have had thicker crusts and more depleted lithospheric mantles than the present (Sleep and Windley, 1982; van Thienen et al., 2004; van Hunen et al., 2008; Hawkesworth et al., 2020), the mechanism described here could have played a more significant role in the early stages of continental growth.

ACKNOWLEDGMENTS

We thank editor Rob Strachan for handling our manuscript. We also thank Lin Chen and two anonymous reviewers for their constructive suggestions and comments. This study is supported by the National Nature Science Foundation of China (granbts 41530319 and 41830212). This work is also related to the International Geoscience Programme IGCP-662.

REFERENCES CITED

Afonso, J.C., Ranalli, G., and Fernández, M., 2007, Density structure and buoyancy of the oceanic lithosphere revisited: *Geophysical Research Letters*, v. 34, L10302, <https://doi.org/10.1029/2007GL029515>.

Bensen, G.D., Ritzwoller, M.H., Barmin, M.P., Levshin, A.L., Lin, F., Moschetti, M.P., Shapiro, N.M., and Yang, Y., 2007, Processing seismic ambient noise data to obtain reliable broad-band surface wave dispersion measurements: *Geophysical Journal International*, v. 169, p. 1239–1260, <https://doi.org/10.1111/j.1365-246X.2007.03374.x>.

Chen, B., and Jahn, B.M., 2004, Genesis of post-collisional granitoids and basement nature of the Junggar Terrane, NW China: Nd-Sr isotope and trace element evidence: *Journal of Asian Earth Sciences*, v. 23, p. 691–703, [https://doi.org/10.1016/S1367-9120\(03\)00118-4](https://doi.org/10.1016/S1367-9120(03)00118-4).

Christensen, N.I., 1996, Poisson's ratio and crustal seismology: *Journal of Geophysical Research*, v. 101, p. 3139–3156, <https://doi.org/10.1029/95JB03446>.

Dewey, J., 2003, Ophiolites and lost oceans: Rifts, ridges, arcs, and/or scrapings?, in Dilek, Y., and Newcomb, S., eds., *Ophiolite Concept and the Evolution of Geological Thought: Geological Society of America Special Paper 373*, p. 153–158, <https://doi.org/10.1130/0-8137-2373-6.153>.

Dilek, Y., and Furnes, H., 2011, Ophiolite genesis and global tectonics: Geochemical and tectonic fingerprinting of ancient oceanic lithosphere: *Geological Society of America Bulletin*, v. 123, p. 387–411, <https://doi.org/10.1130/B30446.1>.

Forsyth, D., and Uyeda, S., 1975, On the relative importance of the driving forces of plate motion: *Geophysical Journal International*, v. 43, p. 163–200, <https://doi.org/10.1111/j.1365-246X.1975.tb00631.x>.

Granot, R., 2016, Palaeozoic oceanic crust preserved beneath the eastern Mediterranean: *Nature Geoscience*, v. 9, p. 701–705, <https://doi.org/10.1038/ngeo2784>.

Hawkesworth, C.J., Cawood, P.A., and Dhuime, B., 2020, The evolution of the continental crust and the onset of plate tectonics: *Frontiers of Earth Science*, v. 8, 326, <https://doi.org/10.3389/feart.2020.00326>.

Morgan, J.P., and Vannucchi, P., 2022, Transmogriification of ocean into continent: Implications for continental evolution: *Proceedings of the National Academy of Sciences of the United States of America*, v. 119, e2122694119, <https://doi.org/10.1073/pnas.2122694119>.

Schiffers, C., Balling, N., Jacobsen, B.H., Stephenson, R.A., and Nielsen, S.B., 2014, Seismological evidence for a fossil subduction zone in the East Greenland Caledonides: *Geology*, v. 42, p. 311–314, <https://doi.org/10.1130/G35244.1>.

Sleep, N.H., and Windley, B.F., 1982, Archean plate tectonics: Constraints and inferences: *The Journal of Geology*, v. 90, p. 363–379, <https://doi.org/10.1086/628691>.

Tang, G.J., Wang, Q., Wyman, D.A., Li, Z.X., Zhao, Z.H., Jia, X.H., and Jiang, Z.Q., 2010, Ridge subduction and crustal growth in the Central Asian Orogenic Belt: Evidence from Late Carboniferous adakites and high-Mg diorites in the western Junggar region, northern Xinjiang (west China): *Chemical Geology*, v. 277, p. 281–300, <https://doi.org/10.1016/j.chemgeo.2010.08.012>.

van Hunen, J., van Keken, P.E., Hynes, A., and Davies, G.F., 2008, Tectonics of early Earth: Some geodynamic considerations, in *Condie, K.C., and Pease, V., eds., When Did Plate Tectonics Begin on Planet Earth?: Geological Society of America Special Paper 440*, p. 157–171, [https://doi.org/10.1130/2008.2440\(08\)](https://doi.org/10.1130/2008.2440(08)).

van Thienen, P., van den Berg, A.P., and Vlaar, N.J., 2004, Production and recycling of oceanic crust in the early Earth: *Tectonophysics*, v. 386, p. 41–65, <https://doi.org/10.1016/j.tecto.2004.04.027>.

Vogt, K., and Gerya, T.V., 2014, From oceanic plateaus to allochthonous terranes: Numerical modelling: *Gondwana Research*, v. 25, p. 494–508, <https://doi.org/10.1016/j.gr.2012.11.002>.

Wang, Y., Forsyth, D.W., Rau, C.J., Carriero, N., Schmandt, B., Gaherty, J.B., and Savage, B., 2013, Fossil slabs attached to unsubducted fragments of the Farallon plate: *Proceedings of the National Academy of Sciences of the United States of America*, v. 110, p. 5342–5346, <https://doi.org/10.1073/pnas.1214880110>.

Watson, M.P., Hayward, A.B., Parkinson, D.N., and Zhang, Z.M., 1987, Plate tectonic history, basin development and petroleum source rock deposition onshore China: *Marine and Petroleum Geology*, v. 4, p. 205–225, [https://doi.org/10.1016/0264-8172\(87\)90045-6](https://doi.org/10.1016/0264-8172(87)90045-6).

Wu, S.C., Huang, R., Xu, Y.X., Yang, Y.J., Jiang, X.H., and Zhu, L.P., 2018, Seismological evidence for a remnant oceanic slab in the Western Junggar, northwest China: *Journal of Geophysical Research: Solid Earth*, v. 123, p. 4157–4170, <https://doi.org/10.1029/2017JB015332>.

Xiao, W.J., Han, C.M., Yuan, C., Sun, M., Lin, S.F., Chen, H.L., Li, Z.L., Li, J.L., and Sun, S., 2008, Middle Cambrian to Permian subduction-related accretionary orogenesis of Northern Xinjiang, NW China: Implications for the tectonic evolution of central Asia: *Journal of Asian Earth Sciences*, v. 32, p. 102–117, <https://doi.org/10.1016/j.jseaes.2007.10.008>.

Xu, Q.Q., Ji, J.Q., Zhao, L., Gong, J.F., Zhou, J., He, G.Q., Zhong, D.L., Wang, J.D., and Griffiths, L., 2013, Tectonic evolution and continental crust growth of Northern Xinjiang in northwestern China: Remnant ocean model: *Earth-Science Reviews*, v. 126, p. 178–205, <https://doi.org/10.1016/j.earscirev.2013.08.005>.

Xu, Y.X., Yang, B., Zhang, S., Liu, Y., Zhu, L.P., Huang, R., Chen, C., Li, Y.T., and Luo, Y.H., 2016, Magnetotelluric imaging of a fossil Paleozoic intraoceanic subduction zone in western Junggar, NW China: *Journal of Geophysical Research: Solid Earth*, v. 121, p. 4103–4117, <https://doi.org/10.1002/2015JB012394>.

Xu, Y.X., Yang, B., Zhang, A.Q., Wu, S.C., Zhu, L., Yang, Y.J., Wang, Q.Y., and Xia, Q.K., 2020, Magnetotelluric imaging of a fossil oceanic plate in northwestern Xinjiang, China: *Geology*, v. 48, p. 385–389, <https://doi.org/10.1130/G47053.1>.

Yan, Z.Y., Chen, L., Xiong, X., Wan, B., and Xu, H.Z., 2021, Oceanic plateau and subduction zone jump: Two-dimensional thermo-mechanical modeling: *Journal of Geophysical Research: Solid Earth*, v. 126, e2021JB021855, <https://doi.org/10.1029/2021JB021855>.

Yang, Y.J., and Forsyth, D.W., 2006, Regional tomographic inversion of the amplitude and phase of Rayleigh waves with 2-D sensitivity kernels: *Geophysical Journal International*, v. 166, p. 1148–1160, <https://doi.org/10.1111/j.1365-246X.2006.02972.x>.

Yang, Y.J., Forsyth, D.W., and Weeraratne, D.S., 2007, Seismic attenuation near the East Pacific Rise and the origin of the low-velocity zone: *Earth and Planetary Science Letters*, v. 258, p. 260–268, <https://doi.org/10.1016/j.epsl.2007.03.040>.

Yin, J.Y., Long, X.P., Yuan, C., Sun, M., Zhao, G.C., and Geng, H.Y., 2013, A Late Carboniferous–Early Permian slab window in the West Junggar of NW China: Geochronological and geochemical evidence from mafic to intermediate dikes: *Lithos*, v. 175–176, p. 146–162, <https://doi.org/10.1016/j.lithos.2013.04.005>.

Zhang, A.Q., Afonso, J.C., Xu, Y.X., Wu, S.C., Yang, Y.J., and Yang, B., 2019, The deep lithospheric structure of the Junggar Terrane, NW China: Implications for its origin and tectonic evolution: *Journal of Geophysical Research: Solid Earth*, v. 124, p. 11,615–11,638, <https://doi.org/10.1029/2019JB018302>.

Zhang, D.H., Huang, B.C., Zhao, G.C., Meert, J.G., Williams, S., Zhao, J., and Zhou, T.H., 2021, Quantifying the extent of the Paleo-Asian Ocean during the Late Carboniferous to Early Permian: *Geophysical Research Letters*, v. 48, e2021GL094498, <https://doi.org/10.1029/2021GL094498>.

Zhao, J.M., Liu, G.D., Lu, Z.X., Zhang, X.K., and Zhao, G.Z., 2003, Lithospheric structure and dynamic processes of the Tianshan orogenic belt and the Junggar basin: *Tectonophysics*, v. 376, p. 199–239, <https://doi.org/10.1016/j.tecto.2003.07.001>.

Zheng, J.P., Sun, M., Zhao, G.C., Robinson, P.T., and Wang, F.Z., 2007, Elemental and Sr-Nd-Pb isotopic geochemistry of Late Paleozoic volcanic rocks beneath the Junggar basin, NW China: Implications for the formation and evolution of the basin basement: *Journal of Asian Earth Sciences*, v. 29, p. 778–794, <https://doi.org/10.1016/j.jseaes.2006.05.004>.

Printed in USA